MOLECULAR AND CELLULAR BIOLOGY, June 2010, p. 2971–2982 Vol. 30, No. 12
0270-7306/10/$12.00 doi:10.1128/MCB.00240-10

TIN2-Tethered TPP1 Recruits Human Telomerase to Telomeres *In Vivo*▽

Eladio Abreu,[1]§ Elena Aritonovska,[2]§ Patrick Reichenbach,[2] Gaël Cristofari,[2]† Brad Culp,[1] Rebecca M. Terns,[1] Joachim Lingner,[2]* and Michael P. Terns[1]*

Departments of Biochemistry and Molecular Biology and Genetics, University of Georgia, Athens, Georgia 30602,[1] and Swiss Institute for Experimental Cancer Research (ISREC), School of Life Sciences, Frontiers in Genetics National Center of Competence in Research, Ecole Polytechnique Fédérale de Lausanne (EPFL), 1015 Lausanne, Switzerland[2]

Received 2 March 2010/Returned for modification 22 March 2010/Accepted 7 April 2010

Recruitment to telomeres is a pivotal step in the function and regulation of human telomerase; however, the molecular basis for recruitment is not known. Here, we have directly investigated the process of telomerase recruitment via fluorescence *in situ* hybridization (FISH) and chromatin immunoprecipitation (ChIP). We find that depletion of two components of the shelterin complex that is found at telomeres—TPP1 and the protein that tethers TPP1 to the complex, TIN2—results in a loss of telomerase recruitment. On the other hand, we find that the majority of the observed telomerase association with telomeres does not require POT1, the shelterin protein that links TPP1 to the single-stranded region of the telomere. Deletion of the oligonucleotide/oligosaccharide binding fold (OB-fold) of TPP1 disrupts telomerase recruitment. In addition, while loss of TPP1 results in the appearance of DNA damage factors at telomeres, the DNA damage response per se does not account for the telomerase recruitment defect observed in the absence of TPP1. Our findings indicate that TIN2-anchored TPP1 plays a major role in the recruitment of telomerase to telomeres in human cells and that recruitment does not depend on POT1 or interaction of the shelterin complex with the single-stranded region of the telomere.

The physical ends of eukaryotic chromosomes, termed telomeres, are maintained by the cellular reverse transcriptase telomerase. Telomerase uses an internal RNA moiety as a template to add short telomeric repeats to the 3′ ends of chromosomes (18, 32). Telomeres protect chromosomes from nucleolytic degradation and inappropriate DNA repair reactions (38). In humans, telomerase is developmentally regulated and is expressed primarily during the first weeks of embryogenesis (10). Later in life, most normal human somatic cells express only very low levels of telomerase, and telomeres shorten with continuous cell division cycles due to the end replication problem and nucleolytic processing of chromosome ends. Upon reaching a critical length, short telomeres activate a DNA damage response that leads to a permanent cell cycle arrest or apoptosis (15). Reactivation of telomerase is a key requisite for human cancer cells to attain unlimited proliferation potential (7). Telomere shortening suppresses tumor formation, but at the same time, the telomere reserve must be long enough to allow tissue renewal by healthy cells during the entire life span (27). Indeed, accelerated telomere shortening causes dyskeratosis congenita, a bone marrow failure syndrome that leads to premature death due to aplastic anemia (47). Telomere dysfunction has also been linked to the pathogenesis of idiopathic pulmonary fibrosis (2), ICF syndrome (55), and Werner syndrome (11).

The maturation and activity of telomerase depend on subcellular trafficking. A minimal, catalytically active telomerase enzyme (that can add telomeric repeats to the ends of DNA oligonucleotide substrates *in vitro*) can be formed by the telomerase reverse transcriptase (TERT) and the telomerase RNA moiety (TR) (3, 49). However, the human TERT (hTERT)-hTR core complex is not competent for telomere elongation *in vivo*. Within cells, hTR accumulates in Cajal bodies (CBs), subnuclear structures that also contain the subset of box H/ACA pseudouridylation guide RNAs termed small CB-specific RNAs (scaRNAs), which modify snRNAs (22, 56). hTR accumulation in Cajal bodies is not needed for assembly of the catalytic core of telomerase but is required to render telomerase competent for telomere association and extension *in vivo* (12, 46). The telomerase holoenzyme subunit TCAB1 (telomerase Cajal body factor 1) mediates the essential CB localization step (46). Telomere synthesis occurs during S phase, and hTR localizes to telomeres specifically during this phase of the cell cycle (23, 44). However, factors that function in the recruitment of telomerase to telomeres are not known.

The six-component telomere capping complex termed shelterin is important for telomere length control *in vivo* (38, 51), suggesting potential roles for the complex in the regulation of telomerase access to telomeres. Interestingly (and perplexingly), current evidence suggests that shelterin components can both inhibit and stimulate telomere elongation. The six shelterin components are TRF1, TRF2, RAP1, TIN2, POT1, and TPP1 (16, 51) (Fig. 1A). The shelterin complex associates with the double-stranded region of the telomere through direct

* Corresponding author. Mailing address for Joachim Lingner: Swiss Institute for Experimental Cancer Research (ISREC), School of Life Sciences, Frontiers in Genetics National Center of Competence in Research, Ecole Polytechnique Fédérale de Lausanne (EPFL), 1015 Lausanne, Switzerland. Phone: 41-(21) 693-0721. Fax: 41-(21) 693-0720. E-mail: joachim.lingner@epfl.ch. Mailing address for Michael P. Terns: Departments of Biochemistry and Molecular Biology and Genetics, University of Georgia, Athens, GA 30602. Phone: (706) 542-1896. Fax: (706) 542-1752. E-mail: mterns@bmb.uga.edu.

† Present address: INSERM U998, CNRS UMR 6267, University of Nice-Sophia-Antipolis, Faculty of Medicine, 06107 Nice, France.

§ These authors contributed equally to this work.

▽ Published ahead of print on 19 April 2010.

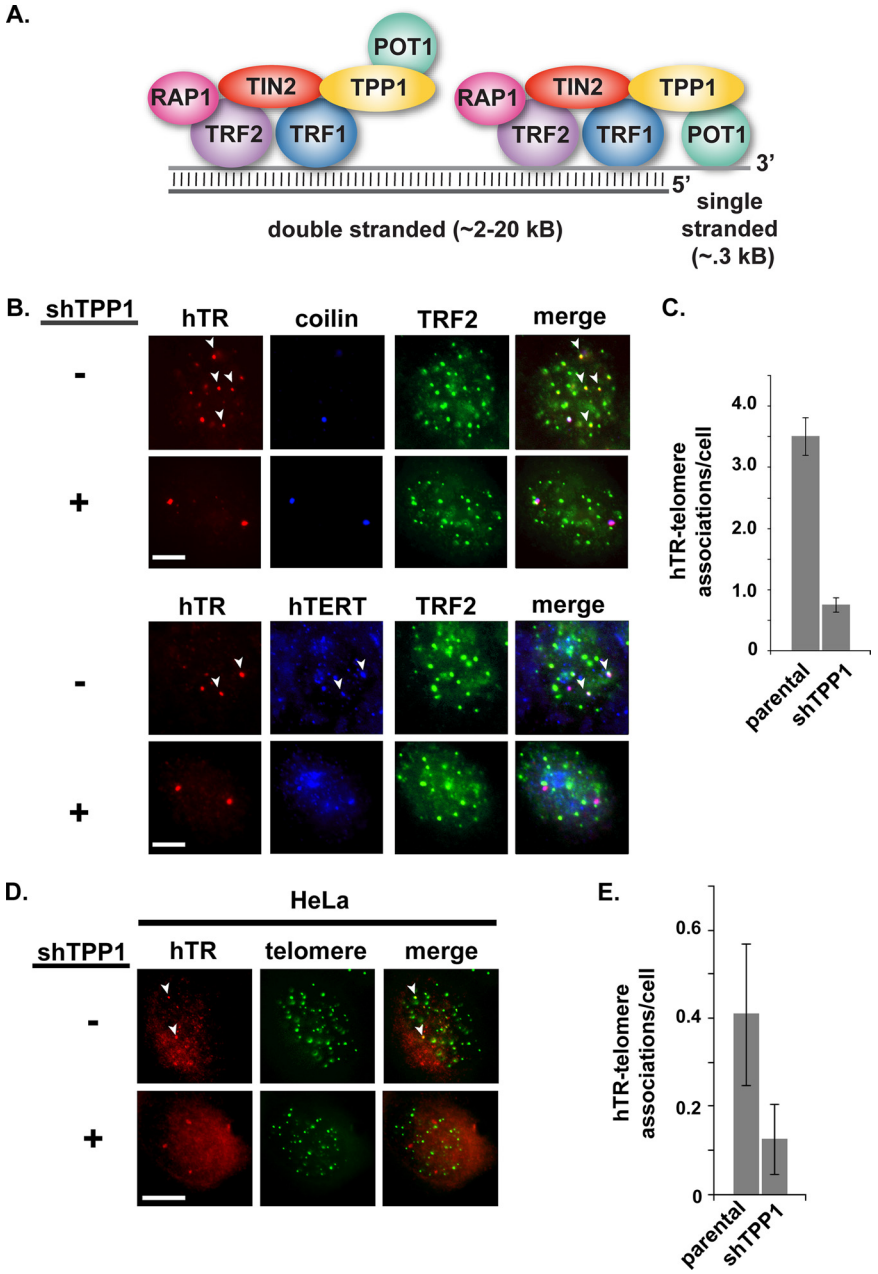

FIG. 1. TPP1 depletion results in loss of localization of telomerase to telomeres (assessed by FISH). (A) Mammalian chromosome end structure is regulated by a complex of six core telomere-associated proteins (indicated) that make up the shelterin complex (16, 51). TPP1 is associated with the double-stranded and single-stranded portion of telomeres via direct interactions with TIN2 and POT1, respectively (16, 51). (B) Fluorescence *in situ* hybridization (FISH) was used to detect hTR (red), and immunofluorescence (IF) was used to detect TRF2 (telomere marker, green) and hTERT (blue) or coilin (Cajal body marker, blue) in parental (−) and TPP1-depleted (+) super-telomerase HeLa cells. Cells were imaged by fluorescence microscopy. Merge panels in all microscopy figures show superimposition of the individual panels. A subset of hTR (hTERT) colocalizations with telomeres is indicated with arrowheads. Scale bars in all microscopy panels represent 10 μm. (C) The average number of hTR-telomere associations per cell (one focal plane) detected by FISH/IF in parental and TPP1-depleted cells represented in panel B is shown. Error bars in plots of localization data in all figures indicate standard errors (see Materials and Methods). (D) Parental (−) and TPP1-depleted (+) HeLa cells (no exogenous telomerase expression) were synchronized to mid-S phase during drug selection. hTR (red) and telomeres (green) were detected by FISH. hTR colocalizations with telomeres are indicated with arrowheads. (E) The average number of hTR-telomere associations per cell (one focal plane) detected by FISH/IF in parental and TPP1-depleted cells represented in panel D is shown.

interactions of TRF1 and TRF2 with the DNA (8, 16). POT1 binds the single-stranded region of the telomere (6, 29). Depletion of TRF1 leads to telomere elongation, and overexpression of TRF1 causes telomere shortening in human telomerase-positive cells without affecting *in vitro*-assayed telomerase activity (41), suggesting that reinforcement of the shelterin complex inhibits telomerase function. Similarly, depletion of TPP1 by RNA interference (RNAi) or disruption of the TPP1-

POT1 interaction (which are both accompanied by loss of the POT1 signal at telomeres) also results in telomere lengthening (33, 54). At the same time, however, several findings support positive roles of shelterin in telomere length regulation. In particular, TPP1 together with POT1 has been shown to improve telomerase activity and processivity *in vitro* (48) by slowing primer dissociation and aiding telomerase translocation (28). Dissection of the apparently opposing roles of the shelterin complex components in telomerase function awaits further investigation.

TPP1 has been hypothesized to play a role specifically in the recruitment of telomerase to telomeres based on its association with telomerase (52). Xin et al. demonstrated that tandem affinity purification (TAP)-tagged hTERT and glutathione *S*-transferase (GST)-tagged TPP1 copurify when fractionated from cellular extracts derived from cells coexpressing the tagged proteins (52). In addition, both GST-tagged TPP1 and the oligonucleotide/oligosaccharide binding fold (OB-fold) of TPP1 pull down *in vitro*-translated hemagglutinin (HA)-tagged TERT and telomerase activity (52), indicating that the TPP1 OB-fold is important for association of TPP1 with telomerase. It is not clear whether the interaction between TPP1 and hTERT is direct. These studies did not examine recruitment of telomerase to telomeres. However, based on their findings, the authors speculated that TPP1 together with POT1 could play a role in positively (and negatively) regulating access of telomerase to telomeres (52).

In this work, we have directly investigated the process of telomerase recruitment using fluorescence *in situ* hybridization (FISH) and immunofluorescence (IF) in parallel with quantitative chromatin immunoprecipitation (ChIP) to monitor the association of hTR and hTERT with telomeres. We find that short hairpin RNA (shRNA)-mediated depletion of TPP1 and TIN2, but not POT1, significantly reduces the presence of telomerase at telomeres. Our findings reveal that TPP1 bound to telomeres via TIN2 plays a key role in the accumulation of telomerase at telomeres.

MATERIALS AND METHODS

Plasmids. shRNA vectors were prepared by cloning double-stranded DNA oligonucleotides into pSuper-Puro (4). The target sequences were as follows: TPP1, 5′-GACUUAGAUGUUCAGAAAA-3′; TIN2, 5′-GTGGAACATTTTC CGCGAGTACTGGAGT-3′ (53); and POT1, 5′-GTACTAGAAGCCTATCTC A-3′ (shRNA 1) and 5′-GGGTGGTACAATTGTCAAT-3′ (shRNA 2). Full-length TPP1, TPP1 lacking the OB-fold (TPP1ΔOB) (52), and full-length TPP1 bearing two silent mutations in the shRNA target site (1575 A→G and 1581 T→A) were eptitope tagged (N-terminal and C-terminal 3×Flag from Sigma) and expressed from pcDNA6 (Invitrogen).

Cell culture and transfection. Super-telomerase HeLa cells were generated as described previously (13). Cells were transfected using Lipofectamine 2000 according to the manufacturer's protocol (Invitrogen). Puromycin (1 μg/ml) (InvivoGen) was added to the medium 24 h after transfection of pSuper-Puro derivatives. Puromycin selection was maintained until mock-transfected cells were dead (approximately 3 days). For TPP1 shRNA- and TIN2 shRNA-treated cells, ChIP analysis was performed 4 days posttransfection. POT1 shRNA-treated cells were analyzed 6 days posttransfection.

For FISH and IF, HeLa cells and super-telomerase HeLa (13) cells were grown on coverslips in Dulbecco modified Eagle medium (DMEM) (Fisher Scientific, Pittsburgh, PA) supplemented with 10% fetal bovine serum (FBS) (Fisher Scientific). All cells were cultured at 37°C with 5% CO_2. Transfections were carried out using Lipofectamine 2000 transfection reagent, according to the manufacturer's protocol (Invitrogen, Carlsbad, CA). Cells were selected in 1 μg/ml puromycin (Sigma-Aldrich) for 48 h following transfection. In some cases, cells were synchronized to mid-S phase using double thymidine block as previously described (44) except that 18-h thymidine treatments were used. (Cells were released for 9 h between thymidine treatments.) Bromodeoxyuridine (BrdU) labeling was performed as described previously (44) to confirm S-phase synchronization.

Fluorescence *in situ* hybridization (FISH) and immunofluorescence (IF). Three DNA probes (probes 1, 2, and 3), complementary to different regions of telomerase RNA, were used in hTR FISH (44). A fourth DNA probe, complementary to the G-rich strand of the telomere (CT*AACCCTAACCCT*AACC CTAACCCT*AACCCTAACCCT*AACCCTAACCCT*A [T* indicates aminoallyl-modified thymidines]), was synthesized by Qiagen (Valencia, CA) and used to detect telomeres. Probes were conjugated with Cy3 or Oregon green monofunctional reactive dye according to the manufacturer's protocol (GE Healthcare, Little Chalfont, Buckinghamshire, United Kingdom; Invitrogen). A 25-ng portion of each Cy3-labeled hTR FISH probe and/or 0.2 ng of telomere FISH probe was used per coverslip. FISH was performed essentially as described previously (44). However, when hTR FISH was performed in combination with BrdU or telomere FISH, the cells were subjected to a 10-min denaturation at 85°C in 70% formamide, 2× SSC (1× SSC is 0.15 M NaCl plus 0.015 M sodium citrate) prior to FISH.

Following FISH, cells were analyzed by IF as described previously (44). Cells were washed three times with 1× phosphate-buffered saline (PBS) and blocked for 1 h in 0.05% Tween-20 in PBS (PBS-T) or 3% bovine serum albumin (BSA) in PBS. Next, cells were incubated with one of several combinations of the following primary antibodies at the indicated dilution for 1 h at room temperature: mouse anti-p80 coilin (1:5,000, II) (1), mouse anti-TRF2 (1:1,000; Imgenex Corp., San Diego, CA), rabbit anti-hTERT (1:400; Rockland, Gilbertsville, PA), mouse anti-FLAG (1:500; Sigma-Aldrich, St. Louis, MO), rabbit anti-RAP1(1:2,000; Novus Biologicals, Littleton, CO), and rabbit anti-53BP1(1:500; Bethyl, Montgomery, TX). Cells were washed three times in 1× PBS and then incubated with secondary antibody (1:100 Cy2-conjugated goat anti-rabbit IgG [H+L], 1:100 Cy2-conjugated goat anti-mouse IgG [H+L], 1:100 Cy5-conjugated goat anti-mouse IgGγ, 1:100 Cy5-conjugated goat anti-rabbit IgG [H+L], 1:100 7-amino-4-methylcoumarin-3-acetic acid [AMCA]-conjugated goat anti-mouse IgG [H+L], or 1:100 AMCA-conjugated goat anti-rabbit IgG [H+L]) (all from Jackson ImmunoResearch Laboratories, West Grove, PA) for 1 h at room temperature. Primary antibodies were diluted in PBS-T or 3% BSA in PBS, while secondary antibodies were diluted in PBS-T only. Cells were subjected to three final 1× PBS washes and mounted in Prolong Gold (Invitrogen).

Microscopy. Slides were analyzed using a Zeiss Axioskop 2 Mot Plus fluorescence microscope (Carl Zeiss Microimaging, Thornwood, NY). Images were acquired at 63× (Plan Apochromat objectives; numerical aperture, 1.4) using a cooled charge-coupled-device ORCA-ER digital camera (Hamamatsu Photonics, Bridgewater, NJ) and IPLab Spectrum software (BioVision Technologies, Inc., Exton, PA). Linear image adjustments were made when necessary using Adobe Photoshop and applied simultaneously to image groups. The colors depicted in the figures do not necessarily correspond to the "colors" of the fluorescent labels used in the experiment. All data are collected in gray scale and converted to the indicated colors using IPLab Spectrum and/or Adobe Photoshop software. Representative cells are shown in all microscopy figure panels. For quantitation of 53BP1 and POT1 IF data, images from treatment groups were normalized (to the same maximum) before analysis. Plots of average numbers of colocalizations observed per cell (one focal plane) show data obtained from 8 to 12 fields of cells for each treatment group processed in parallel on the same day. Error bars indicate standard errors calculated with *N* equal to the number of fields quantitated.

Chromatin immunoprecipitation. ChIP assays were performed as described previously (13), with the following modifications. For immunoprecipitations, 25 μl of hTERT R484 rabbit serum (50), 2.5 μg mouse monoclonal TPP1 antibody (ACD; Abnova H00065057-M02), or 2 μg mouse monoclonal γH2AX antibody (Millipore 05-636) was used, and the mixtures were incubated for 6 h at 4°C with 50 μl of a 50% slurry of protein A/G-Sepharose beads (GE Healthcare). Telomeric DNA was detected as described previously (5). For detection of Alu sequences, a 5′ ^{32}P-labeled oligonucleotide probe (5′-GTGATCCGCCCGCCT CGGCCTCCCAAAGTG-3′) was used.

qRT-PCR. Total RNA was isolated using TRIzol reagent (Invitrogen). The isolated RNA fraction was treated with RNase-free DNase (Qiagen) and repurified with the TRIzol LS reagent (Invitrogen). For quantitative reverse transcriptase PCR (qRT-PCR), cDNA was prepared from 2 μg total RNA, using random primers and SuperScript III reverse transcription (Invitrogen) followed by qPCR on a 7900HT fast real-time PCR system (Applied Biosystems), using the PowerSYBR Green PCR master mix (Applied Biosystems). For PCR amplification of TIN2 cDNA, forward and reverse primers were 5′-GTCAGAGG CTCCTGTGGATT-3′ and 5′-CAGTGCTTTCTCCAGCTGAC-3′, respectively; POT1 cDNA was amplified with previously described primers (26). Serial

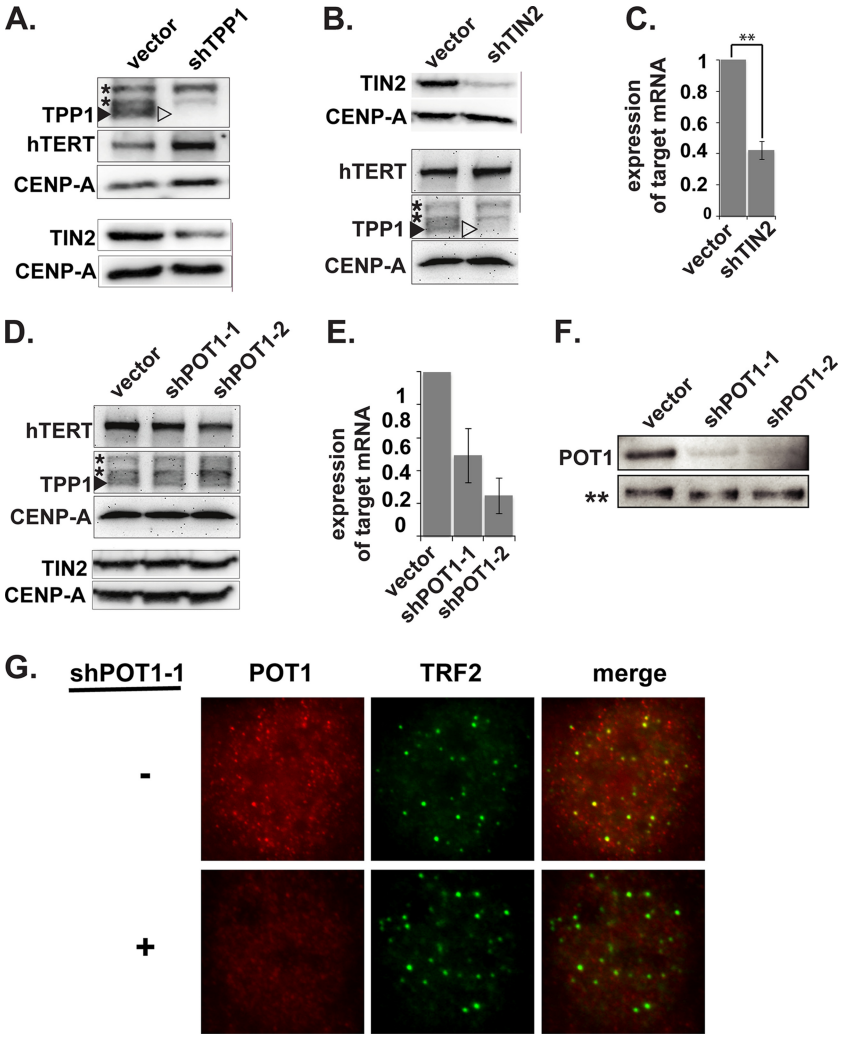

FIG. 2. Depletion of TPP1, TIN2, and POT1. (A) Immunoblot analysis of TPP1-depleted cells. Super-telomerase HeLa cells were transfected with pSuper-Puro (vector) or pSuper-Puro-TPP1 shRNA vector (shTPP1). Four days after transfection, TPP1, hTERT, TIN2, and CENP-A expression was analyzed by immunoblotting. The arrowheads indicate the position of endogenous TPP1 protein. Asterisks indicate nonspecific bands. CENP-A was used as a loading control. (B) Immunoblot analysis of TIN2-depleted cells. Four days after transfection, protein expression was analyzed as described for panel A. (C) qRT-PCR analysis of TIN2-depleted cells. qRT-PCR detection of mRNA levels of TIN2 in super-telomerase HeLa cells, 4 days after transfection with TIN2-shRNA, relative to empty-vector control. Error bars correspond to standard deviations of results of three independent experiments. Statistical analyses were done using a two-tailed Student's t test (**, $P < 0.01$). (D) Immunoblot analysis of POT1-depleted cells. Six days after transfection, protein expression was analyzed as described for panel A. (E) qRT-PCR analysis of POT1-depleted cells. qRT-PCR showing mRNA levels of POT1 in super-telomerase HeLa cells, 6 days after transfection with two different POT1-shRNAs, relative to empty-vector control. Error bars correspond to standard deviations of results of two independent experiments. (F) IP/immunoblot analysis of POT1-depleted cells. Coimmunoprecipitation of endogenous POT1 with TPP1 in POT1-depleted cells. TPP1-immunoprecipitated complexes from super-telomerase HeLa cells transfected with the indicated plasmids were resolved by 8% SDS-PAGE. Immunoblot antibodies are indicated on the left. No detection of TPP1 was observed in the supernatant fraction after IP (data not shown). A nonspecific band recognized by the TPP1 antibody in the IP fraction (**) served as a loading control. (G) Direct IF analysis of POT1-depleted cells. POT1 (red) and TRF2 (green) were detected by IF in parental (−) and POT1-depleted cells.

dilutions of TIN2 and POT1 cDNAs were used to determine amplification efficiencies. TIN2 and POT1 quantities were normalized to the level of β-actin cDNA.

Immunoblots. A total of 5×10^4 cells (or 1×10^4 cells for FLAG immunoblots) were boiled for 5 min in Laemmli loading buffer and fractionated on 4 to 20% SDS-polyacrylamide gradient gels (Lonza) except for TIN2 (10% polyacrylamide gel) and POT1 (8% polyacrylamide gel). Standard immunoblot protocols were used with the following antibodies: mouse monoclonal TPP1 antibody, ACD Abnova H00065057-M02 (1:1,000); rabbit polyclonal TIN2C 701 antibody, a kind gift from S. Smith (1:1,000); rabbit polyclonal hPOT1 978 antibody, a kind gift from T. de Lange (1:1,000); rabbit polyclonal hTERT antibody, Rockland 600-401-252 (1:2,500); rabbit polyclonal CENP-A antibody, Upstate 07-240 (1:2,000); mouse monoclonal γ-H2AX antibody, Millipore 05-636 (1:2,000); and mouse monoclonal FLAG M2 antibody, Sigma F3165 (1:5,000). For POT1 immunoblots, guanidine renaturation was performed as described previously (34). Secondary horseradish peroxidase-conjugated goat antibodies against rabbit or mouse IgG (1:3,000; Promega) were used to reveal the primary antibodies. The AlphaInnotech chemiluminescence substrate and imaging system was used for signal detection and quantification.

Coimmunoprecipitation. Coimmunoprecipitation of endogenous TPP1 and POT1 proteins was performed in super-telomerase HeLa cells transfected with two different shRNAs against POT1. Precleared cell lysates from 10^6 cells were prepared as previously described (34). Lysates were immunoprecipitated with 10 μg mouse monoclonal TPP1 antibody ACD Abnova H00065057-M02, and immune complexes were bound to a 50% slurry of protein G-Sepharose beads. After an overnight

incubation at 4°C, beads were washed four times with lysis buffer (34) and proteins were eluted with Laemmli loading buffer for analysis by 8% SDS-PAGE.

Real-time quantitative telomeric repeat amplification protocol (RQ-TRAP). Telomerase activity was measured as previously described (13), with the following modifications. Reaction mixtures containing the PowerSYBR Green PCR master mix (Applied Biosystems), 1.8 μg undiluted or 3-fold-diluted cell extracts, 1 μM telomerase primer TS, 0.3 μM reverse primer ACX, and 0.5 mM $MgCl_2$ were incubated for 30 min at 30°C and for 10 min at 95°C. Using the 7900HT fast real-time PCR System (Applied Biosystems), samples were amplified in 40 PCR cycles for 15 s at 95°C and 1 min at 60°C. Threefold serial dilutions of the empty-vector-transfected samples were used to obtain a standard curve of the form $\log_{10}$ (protein quantity) = $aC_T + b$, where C_T is the threshold constant, a is the slope of the curve, and b is the y intercept. Telomerase activity was expressed relative to this standard as the quantity of standard sample extract giving the same C_T value. All samples were serially diluted to verify the linearity of the RQ-TRAP reaction and heat inactivated to verify that the amplification product was attributable to telomerase activity.

RESULTS

TPP1 depletion results in loss of association of telomerase with telomeres. The recruitment of telomerase to telomeres is essential for telomere maintenance; however, the mechanism of recruitment is not known. Association of telomerase with telomeres can be observed in cancer cells during S phase by FISH with oligonucleotide probes complementary to hTR or IF with hTERT antibodies (12, 22, 23, 43, 44, 46, 56). Analysis of telomerase recruitment is facilitated by the use of so-called super-telomerase cells, which concomitantly overexpress hTERT and hTR, allowing detection of telomerase association with telomeres by ChIP as well as by microscopy in all phases of the cell cycle (12, 13). In order to identify proteins that are necessary for recruitment of telomerase to telomeres, we depleted candidate recruitment factors using shRNAs in super-telomerase HeLa cells and examined the localization of telomerase by FISH and ChIP analysis. We found that shRNA-induced depletion of the shelterin component TPP1 (Fig. 2A) caused a striking loss of telomerase localization to telomeres as assessed by FISH (Fig. 1) and ChIP (Fig. 3).

In untreated super-telomerase cells, hTR (visualized by FISH) is found at the Cajal bodies (visualized via the Cajal body marker protein coilin) and numerous telomeres (visualized via the telomere-binding protein TRF2) (Fig. 1B, −shTPP1; a subset of the hTR-telomere colocalizations is indicated with arrowheads). Following TPP1 depletion, hTR remains at Cajal bodies but is found only at very few telomeres (Fig. 1B and C, +shTPP1). TPP1 depletion reduced the number of observed hTR-telomere colocalizations by 77%, from a mean of 3.5 ± 0.3 (standard error of the mean [SEM]) colocalizations per cell (one focal plane) in parental super-telomerase cells to 0.8 ± 0.1 (SEM) after TPP1 depletion (Fig. 1C). hTERT localization to telomeres was also noticeably reduced by depletion of TPP1 (Fig. 1B, lower panels; a subset of hTR-hTERT-telomere colocalizations is indicated with arrowheads). At the same time, progression through the cell cycle (assessed by percentage of cells found in S phase), cellular telomerase levels (assayed *in vitro* by RQ-TRAP), and hTERT protein levels (assayed by immunoblot analysis) were not affected by TPP1 depletion (Fig. 2A and data not shown). These results suggest that TPP1 is necessary for the recruitment of telomerase from Cajal bodies to telomeres in super-telomerase cells. Importantly, TPP1 depletion results in a similar loss of hTR localization to telomeres during S phase in standard HeLa cells (not expressing exogenous telomerase) (Fig. 1D and E; telomeres are detected with a DNA probe; a subset of hTR-telomere colocalizations is indicated with arrowheads). TPP1 depletion reduced the number of hTR-telomere colocalizations by 68%, from a mean of 0.41 ± 0.16 (SEM) per cell to 0.13 ± 0.08 (SEM) after TPP1 depletion (Fig. 1E).

We also examined telomerase recruitment to telomeric DNA by ChIP in super-telomerase HeLa cells (Fig. 3). ChIP relies on formaldehyde-mediated covalent linkage of proteins to DNA and therefore reflects close physical as well as spatial

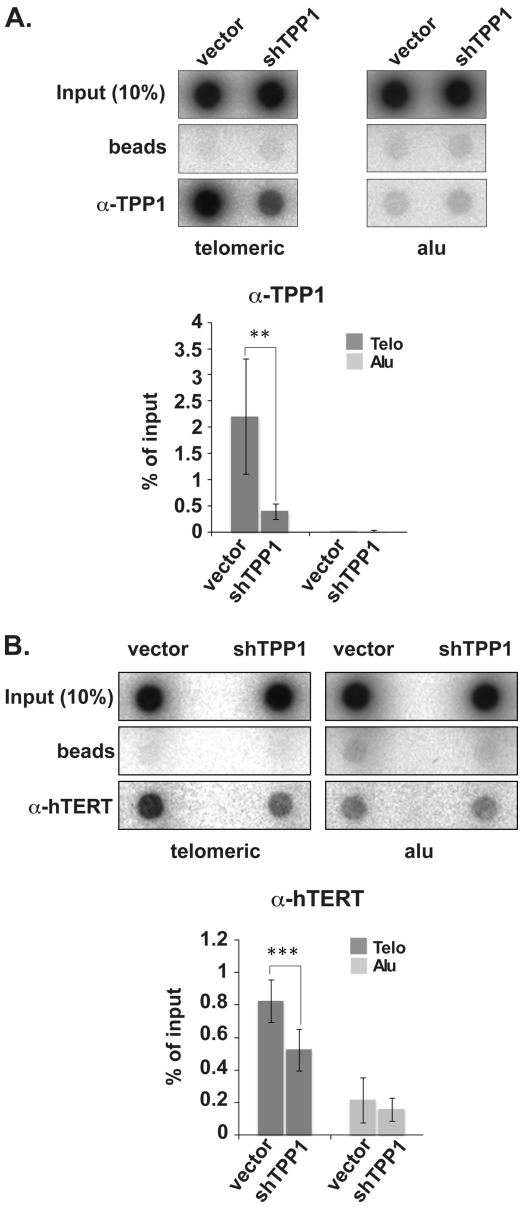

FIG. 3. TPP1 depletion results in loss of physical association of hTERT with telomeres (assessed by ChIP). (A) ChIP of telomeric and Alu DNA with TPP1-specific (A) and hTERT-specific (B) antibodies in super-telomerase HeLa cells. The percentage of telomeric and Alu DNA recovered in each ChIP is indicated. Error bars correspond to standard deviations of results of three (hTERT ChIP) and five (TPP1 ChIP) independent experiments. Statistical analyses were done using a two-tailed Student's t test (***, $P < 0.001$; **, $P < 0.01$).

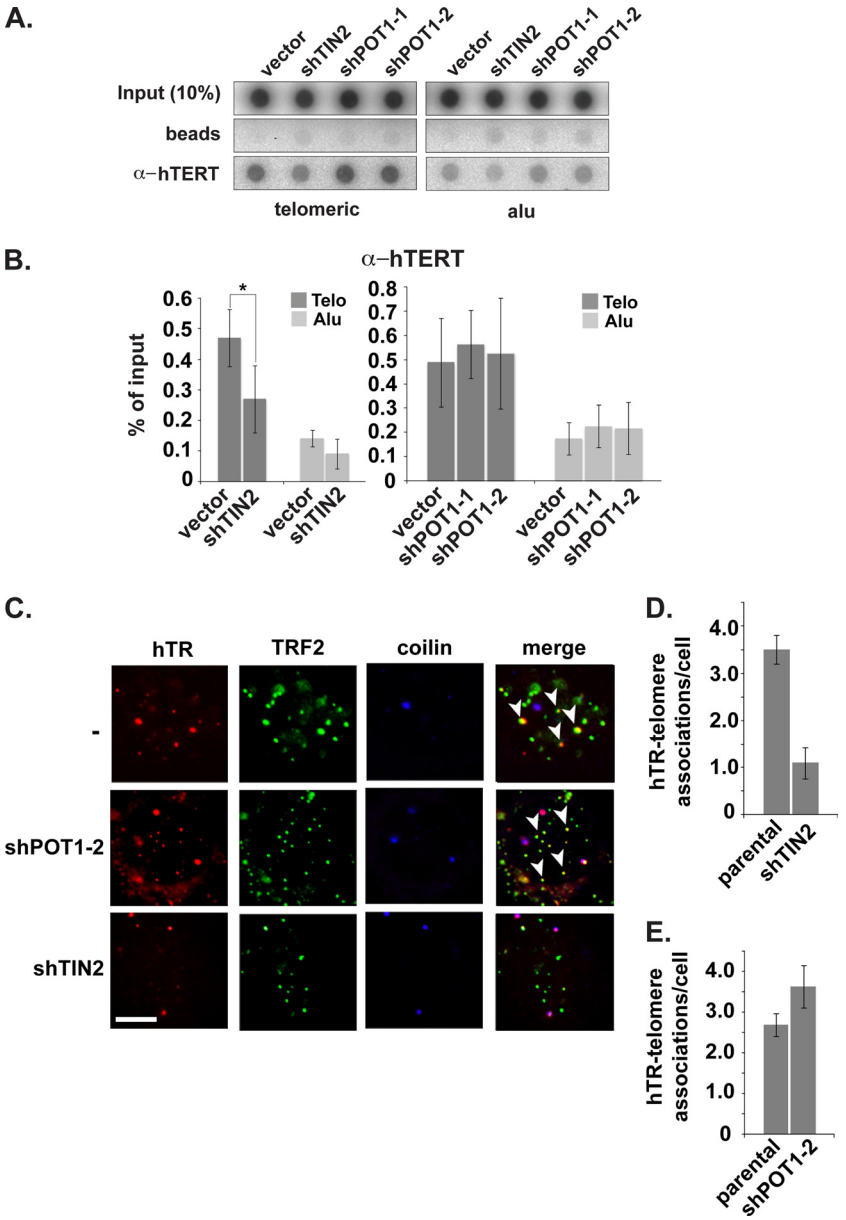

FIG. 4. Telomerase recruitment depends on TIN2 but not POT1. (A) ChIP of telomeric and Alu DNA with hTERT antibody. (B) Quantification of ChIP data shown in panel A. Error bars correspond to standard deviations of results of three (TIN2 data) and two (POT1 data) independent experiments. Statistical analyses were done using a one-tailed Student's *t* test (*, $P < 0.05$). (C) hTR (red) was detected by FISH and TRF2 (green) and coilin (blue) were detected by IF in parental (−) and POT1- or TIN2-depleted cells. hTR colocalizations with telomeres are indicated with arrowheads. (D and E) The average number of hTR-telomere associations per cell (one focal plane) detected by FISH/IF in parental and POT1- or TIN2-depleted cells represented in panel C is shown.

associations of proteins and DNA. TPP1 was depleted (Fig. 2), and the association of telomerase with telomeres (and Alu repeats) was assessed by IP with hTERT antibodies. As expected, little telomeric DNA was immunoprecipitated with TPP1 antibodies upon depletion of TPP1 (Fig. 3A). In addition, however, immunoprecipitation of telomeric DNA with hTERT antibodies was reduced by 36% when cellular TPP1 was depleted (Fig. 3B). The small degree of association of hTERT observed with Alu-repeat DNA, which served as a negative control, was not affected by TPP1 depletion. Thus, both FISH and ChIP analyses implicate TPP1 as a telomerase recruitment factor.

POT1 is not required for association of telomerase with telomeres, but depletion of TIN2 results in reduced association. TPP1 interacts with telomeres via two proteins: TIN2, which binds to the double-stranded telomere-bound TRF1 and TRF2 proteins, and POT1, which mediates interaction with the single-stranded region of the telomere (16, 51) (see Fig. 1A). We found that TPP1 depletion reduced TIN2 protein levels (Fig. 2A), suggesting that the recruitment defect that we ob-

served in TPP1-depleted cells may require TIN2. At the same time, a current model suggests that TPP1 functions with POT1 to recruit telomerase to telomeres (52). To further investigate the mechanism of TPP1-mediated telomerase recruitment, we depleted TIN2 or POT1 using shRNAs (Fig. 2B to G). ChIP analysis indicated that association of hTERT with telomeres was reduced 43% upon depletion of TIN2 (Fig. 4A and B), similar to the reduction observed with TPP1 depletion (Fig. 3). However, immunoblot analysis revealed that depletion of TIN2 also resulted in a reduction in TPP1 protein levels (but not telomerase activity or hTERT protein levels) (Fig. 2B and data not shown). On the other hand, POT1 depletion did not detectably change TPP1 levels (Fig. 2D). In addition, POT1 depletion did not disrupt hTERT association with telomeres in ChIP analysis (Fig. 4A and B).

FISH analysis of hTR also showed a marked difference in the effects of TIN2 and POT1 depletion. hTR-telomere colocalization with TIN2 depletion was reduced to an extent similar to that observed with TPP1 depletion (Fig. 4C and D). Following TIN2 depletion, hTR-telomere colocalizations decreased by 69%, from a mean of 3.5 ± 0.3 (SEM) per cell to 1.1 ± 0.3 (SEM) per cell (Fig. 4D). However, POT1 depletion did not reduce the colocalization of hTR with telomeres (Fig. 4C and E). The results indicate that POT1 and association with the single-stranded region of the telomere (see Fig. 1A) are not required for the association of the majority of telomerase with telomeres and suggest a role for TIN2-tethered TPP1 in recruitment.

The OB-fold of TPP1 is required for association of telomerase with telomeres. In order to further investigate the function of TPP1 in telomerase recruitment, we rescued the shRNA-mediated depletion of endogenous TPP1 by expression of FLAG epitope-tagged TPP1. Control (empty vector) and rescue (TPP1) plasmids were cotransfected along with the TPP1 shRNA-encoding plasmid. Expression of endogenous and exogenous TPP1 was assessed by immunoblot analysis with TPP1 and FLAG antibodies 4 days following transfection (Fig. 5A). The reduction in association of telomerase with telomeres observed with TPP1 depletion by ChIP analysis was not rescued by expression of an shRNA-sensitive TPP1 gene (Fig. 5B and C); in both cases, the telomeric DNA precipitated with hTERT antibody was approximately 50% of the shRNA-negative control. However, expression of an shRNA-resistant TPP1 gene (TPP1*, shRNA mRNA recognition site destroyed without altering the protein sequence) encoding full-length FLAG-tagged TPP1 fully restored telomerase association, indicating that the phenotype is related to TPP1 depletion. In order to test the potential role of the N-terminal OB-fold domain of TPP1 (required for coprecipitation of telomerase and TPP1 in pulldown experiments) (52) in recruitment to telomeres, we introduced an shRNA-resistant truncated version of TPP1 (TPP1ΔOB*). TPP1 lacking the OB-fold did not rescue telomerase recruitment assessed by ChIP (Fig. 5B and C).

At the cellular level, we also observed that cotransfection of shRNA-resistant full-length TPP1 (TPP1*) restored localization of hTR to telomeres (localized via telomere-binding protein TRF2 or RAP1) (Fig. 6A). The FLAG-tagged TPP1 localized to telomeres, including those where hTR was found (Fig. 6A; see arrowheads, TPP1*). Expression of the shRNA-resistant TPP1 increased the number of hTR-telomere colocalizations from a mean of 0.7 ± 0.1 (SEM) per cell, observed in TPP1-depleted cells, to 2.4 ± 0.4 (SEM) per cell, similar to the 2.1 ± 0.3 (SEM) colocalizations per cell observed in parental super-telomerase cells in this experiment (Fig. 6B). On the other hand, TPP1 lacking the OB-fold domain was unable to rescue telomerase recruitment (0.3 ± 0.1 [SEM] hTR-telomere colocalizations per cell) (Fig. 6B), despite the fact that the TPP1ΔOB protein localized to telomeres (see FLAG and RAP1 in Fig. 6A). These results suggest that the association of

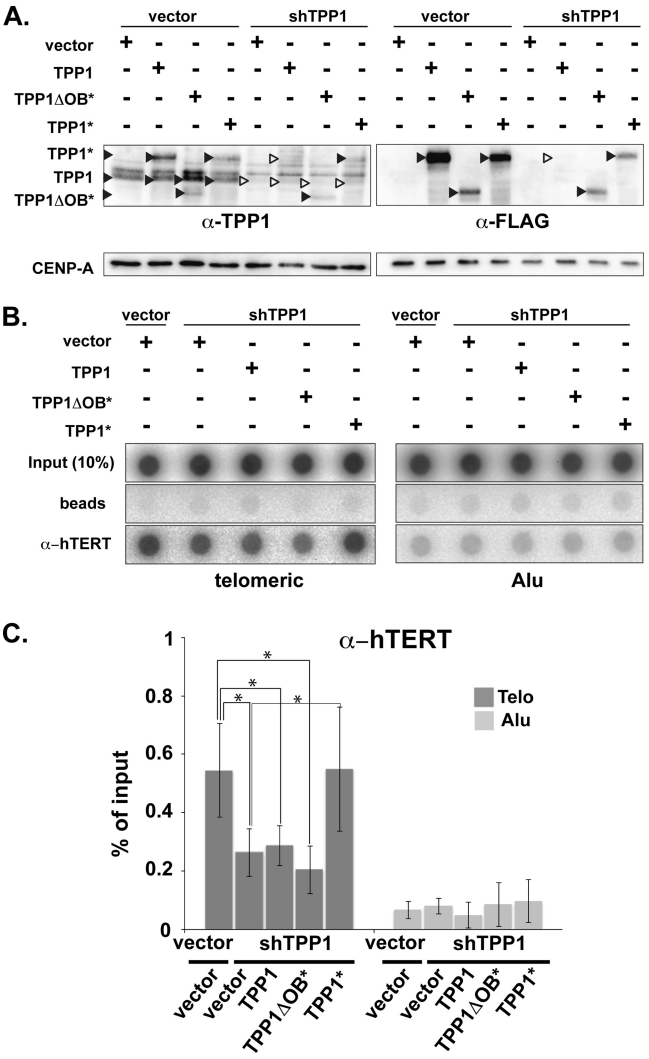

FIG. 5. Human telomerase is recruited to telomeres via the OB-fold of TPP1. (A) Immunoblot analysis of ectopically expressed FLAG epitope-tagged full-length TPP1 (TPP1), FLAG-tagged, shRNA-resistant full-length TPP1 (TPP1∗), and FLAG-tagged, shRNA-resistant TPP1 lacking the OB-fold (TPP1ΔOB∗). Super-telomerase HeLa cells were cotransfected with the indicated plasmids, and protein expression was analyzed 4 days after transfection. Black arrowheads indicate the presence of the respective TPP1 proteins, and white arrowheads indicate the lack of expression. Immunoblots were probed with anti-TPP1, anti-FLAG and CENP-A antibodies as indicated. (B) ChIP of telomeric and Alu DNA with hTERT antibody from cells in panel A. (C) Quantification of data in panel B representing percentage of telomeric and Alu DNA recovered in hTERT ChIP. Error bars correspond to standard deviations of results of four independent experiments. Statistical analyses were done using a two-tailed Student's *t* test (∗, $P < 0.05$).

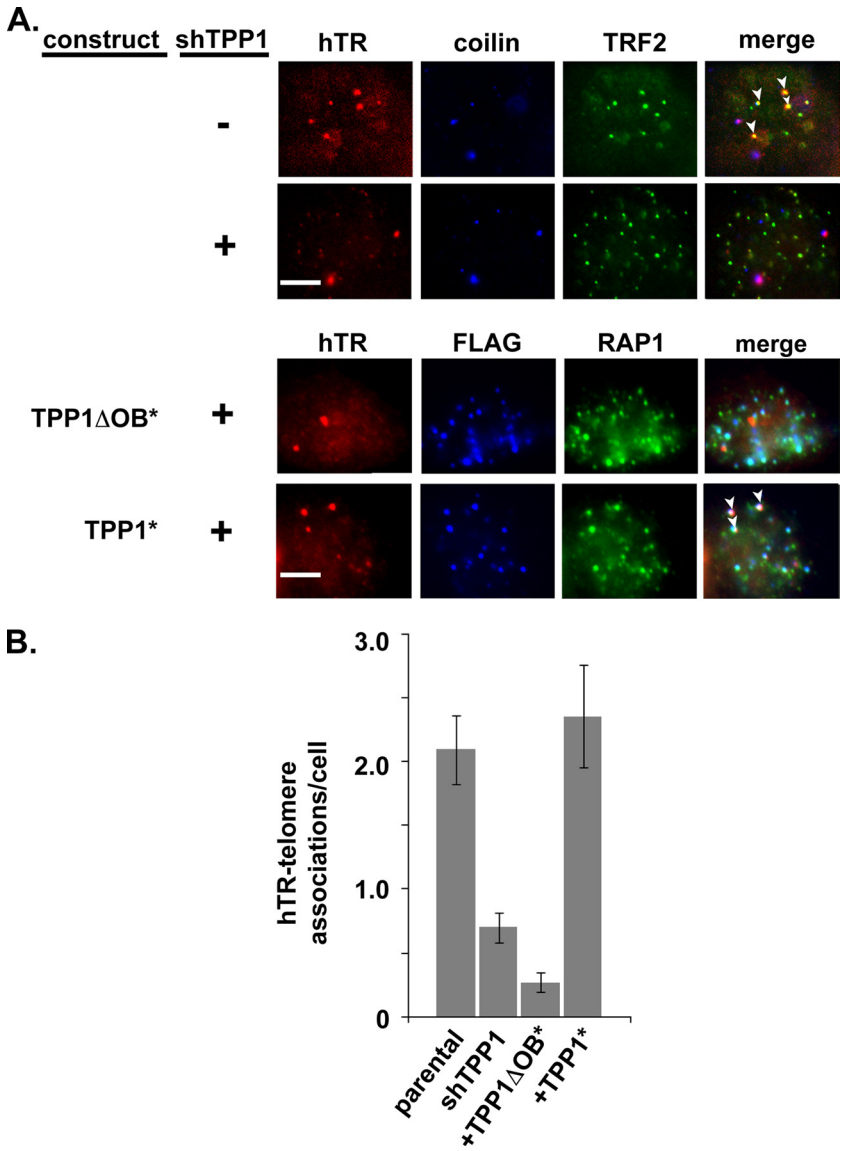

FIG. 6. The TPP1 OB-fold is required to rescue telomerase recruitment to telomeres. An shRNA-resistant form of TPP1 is able to restore hTR localization to telomeres in TPP1-depleted cells. However, an shRNA-resistant form of TPP1 lacking the OB-fold cannot restore localization. (A) Parental and TPP1-depleted super-telomerase HeLa cells were subjected to FISH and IF to detect hTR (red), coilin (blue), and TRF2 (green). Merge panels show superimposition of hTR, coilin, and TRF2. Next, parental cells were cotransfected with shTPP1 and either TPP1∗ or TPP1ΔOB∗. Treated cells were subjected to FISH and IF to detect hTR (red), FLAG (blue), and RAP1 (telomere marker, green). Merge panels show superimposition of hTR, FLAG, and RAP1. (B) Plot of the average number of telomere-associated hTR foci per cell in the parental cells and each experimental group. Error bars indicate standard errors calculated with *N* equal to the number of samples quantitated.

TPP1 and telomerase, which is mediated by the OB-fold of TPP1 (52), functions in recruitment of telomerase to telomeres.

TIF formation does not impair association of telomerase with telomeres. Previous studies demonstrated that depletion of TPP1 activates a DNA damage response marked by the formation of telomere dysfunction-induced foci (TIFs) at telomeres (19, 20, 52). TIF formation can be detected via the association of DNA damage proteins, such as γ-H2AX and 53BP1, with telomeres (42). Accordingly, our ChIP analysis of telomeric DNA with antibodies against the DNA damage marker γ-H2AX revealed a 7-fold increase in γ-H2AX at telomeres when TPP1 levels are reduced (Fig. 7A and B) (without a detectable change in cellular γ-H2AX levels; Fig. 7C). In addition, we found the DNA damage marker 53BP1 at telomeres in 29% ± 8% (SEM) of cells by IF when TPP1 was depleted, relative to 0.4% ± 0.4% (SEM) of untreated cells in our experiments (Fig. 7D) (scoring threshold = 7 or more 53BP1-telomere colocalizations per cell, similar to that used by others [17, 24]). These findings support the previous observations of TIF formation in response to TPP1 depletion and suggest general effects of TPP1 knockdown on telomere composition that could lead to the observed loss of telomerase recruitment. However, additional observations indicate that TIF formation per se does not account for the loss of telomerase recruitment observed in the absence of TPP1.

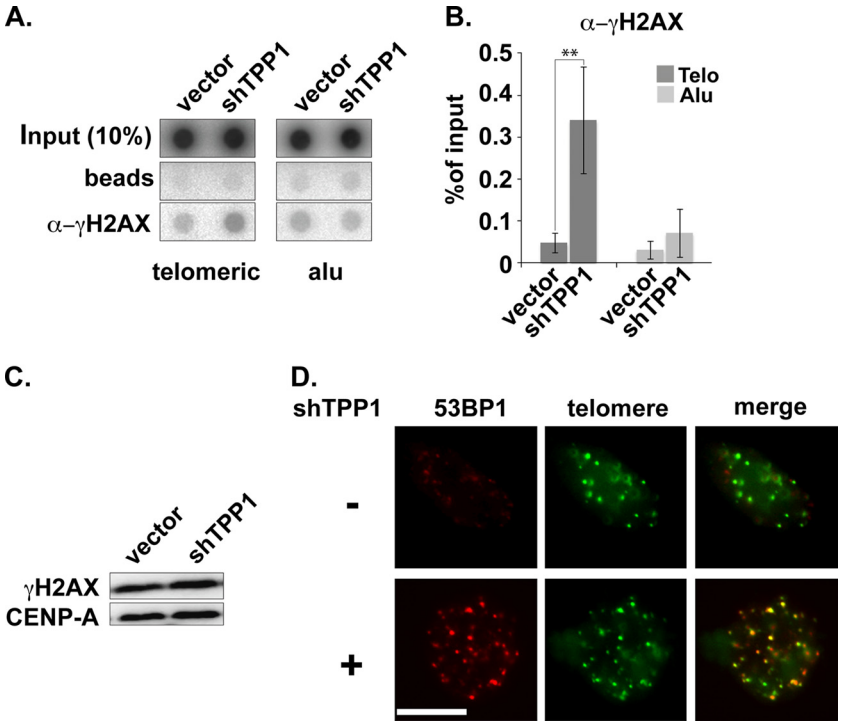

FIG. 7. DNA damage response at telomeres following TPP1 depletion. (A) ChIP of telomeric and Alu DNA with γ-H2AX antibodies. Transfected plasmids are indicated. (B) The graph represents the quantification of the dot blot indicating the percentages of telomeric and Alu DNA recovered with γ-H2AX antibodies. Error bars correspond to standard deviations of four independent experiments. Statistical analyses were done using a two-tailed Student's *t* test (**, $P < 0.01$). (C) Immunoblot was probed with anti-γ-H2AX and CENP-A antibodies following transfection of super-telomerase HeLa cells with empty vector or TPP1 shRNA construct as indicated. (D) TPP1-depleted cells were subjected to FISH and IF to label for telomeres (green) and 53BP1 (TIF marker, red). Merge panels show superimposition of telomeres and 53BP1 (colocalizations are indicated by yellow).

Depletion of POT1 (and TIN2) also leads to a DNA damage response at telomeres (21, 25), evidenced by an increase in γ-H2AX association with telomeric DNA by ChIP analysis (6-fold increase in TIN2-depleted cells and 8- to 10-fold increase in POT1-depleted cells) (Fig. 8). However, the DNA damage response associated with POT1 depletion does not disrupt recruitment of telomerase to telomeres (Fig. 4). In addition, we found that TIFs remained in our cells rescued with the wild-type TPP1 construct. ChIP analysis of γ-H2AX suggests that the TIF formation that occurred with TPP1 depletion was only partially rescued by the full-length TPP1 (or by the TPP1ΔOB protein) under the conditions of the experiment (TPP1*; Fig. 9A and B). (The incomplete suppression of TIFs may reflect lower expression levels of transgenic TPP1 than of endogenous TPP1 [Fig. 5A, lanes 1 and 8].) Moreover, in microscopy experiments, 53BP1 was found at telomeres in 19% ± 6% (SEM) of cells rescued with full-length TPP1 (Fig. 9C) where telomerase recruitment was restored (Fig. 5 and 6) (compared to 0.4% ± 0.4% [SEM] of untreated cells), suggesting that the loss of telomerase recruitment is not a result of secondary effects of TPP1 knockdown on telomere structure. In fact, telomerase was observed at the same telomeres as the TIF marker protein 53BP1 in the rescued cells (Fig. 9C), clearly indicating that TIF formation does not prevent recruitment of telomerase. At the same time, TIFs (indicated by the presence of γ-H2AX or 53BP1 at telomeres) were present in

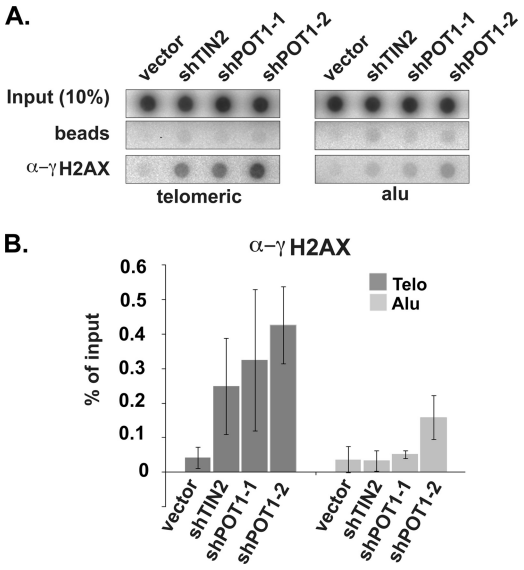

FIG. 8. Increased DNA damage response at telomeres upon TIN2 or POT1 depletion. (A) ChIP of telomeric and Alu DNA with γ-H2AX antibodies. (B) The graph represents the quantification of the dot blot. Error bars correspond to standard deviations of results of two independent experiments.

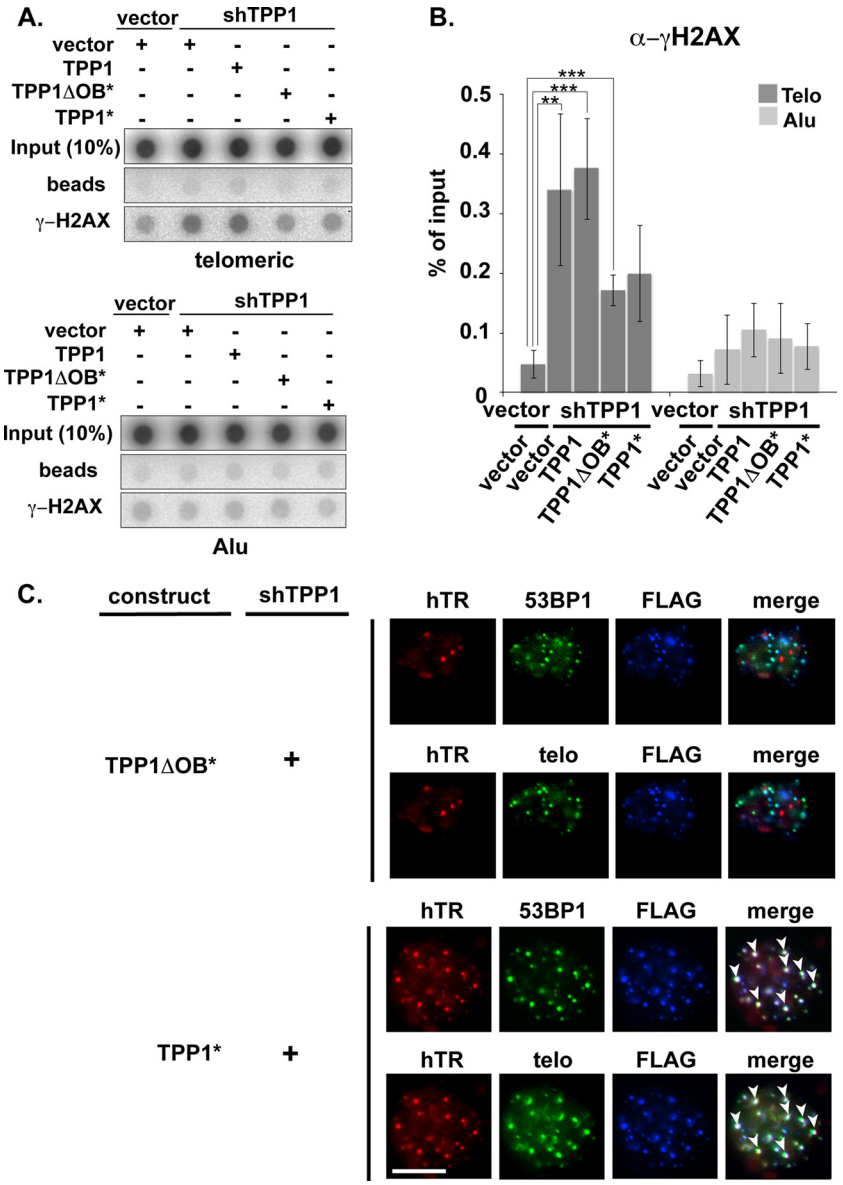

FIG. 9. The presence of TIFs (telomere dysfunction-induced foci) does not impact the ability of TPP1 to rescue telomerase associations with telomeres. (A) ChIP of telomeric and Alu DNA with γ-H2AX antibodies. Transfected plasmids are indicated. Expression of TPP1∗ and TPP1ΔOB∗ partially rescues TIF formation observed in TPP1-depleted cells. (B) The graph represents the quantification of the dot blot indicating the percentages of telomeric and Alu DNA recovered with γ-H2AX antibodies. Error bars correspond to standard deviations of results of four independent experiments. Statistical analyses were done using a two-tailed Student's *t* test (∗∗∗, $P < 0.001$; ∗∗, $P < 0.01$). (C) Although TIFs were detected in TPP1-depleted cells coexpressing TPP1∗ or TPP1ΔOB∗, TIFs did not inhibit rescue of hTR recruitment to telomeres by TPP1∗. Super-telomerase HeLa cells were cotransfected with shTPP1 and either TPP1∗ or TPP1ΔOB∗. Treated cells were subjected to FISH and IF to label for hTR (red), FLAG (blue), 53BP1 (green), and telomeres (green). Merge panels show superimposition of hTR, 53BP1, and FLAG or hTR, telomeres, and FLAG.

cells depleted of TPP1 (Fig. 7) or expressing the TPP1ΔOB protein (Fig. 9), indicating that the DNA damage response at telomeres also does not stimulate telomerase recruitment in the absence of intact TPP1. The results indicate that the association of telomerase with telomeres depends on TPP1 and, in particular, on the OB-fold domain of TPP1.

DISCUSSION

It is now clear that one primary mechanism for the regulation of telomerase activity is through regulated intracellular trafficking of the enzyme (23, 43, 44). Accumulation of hTR in Cajal bodies is mediated by TCAB1 and is required to render telomerase competent for association with telomeres in the S phase of the cell cycle (12, 46). The factors responsible for the recruitment of telomerase to telomeres have remained unidentified. In this study, using combined FISH and ChIP analysis, we have determined that depletion of shelterin proteins TPP1 and TIN2 (but not POT1) prevents association of telomerase with telomeres (Fig. 1 and 3). These findings indicate that the majority of telomerase is recruited to telomeres by TPP1,

which is bound to telomeres via TIN2 in humans and likely other vertebrates (see Fig. 1A).

TPP1 could theoretically function in telomerase recruitment specifically when bound to the single-stranded 3′ region of the telomere via POT1 (14, 16, 38, 51) (Fig. 1A). Indeed, TPP1 has been speculated to function with POT1 to recruit telomerase (52). However, we did not detect significant changes in telomerase recruitment upon depletion of POT1 (Fig. 4), indicating that interaction with POT1 and the single-stranded end of the telomere is not required for recruitment of telomerase to telomeres by TPP1. At the same time, our results do not exclude the possibility that POT1 also plays an important role (positive or negative) in telomerase recruitment. The single-stranded 3′ overhang of the telomere is generally much less extensive (typically 0.1 to 0.3 kb) than the double-stranded tract (typically 2 to 20 kb), and thus the fraction of telomerase that may be present at the 3′ overhang would be expected to be small relative to that bound to the double-stranded part of the telomere. A specific change in telomerase levels at the single-stranded end may be difficult to detect above the background of telomerase associated with the rest of the telomere. Logically, the association of telomerase with the single-stranded region of the telomere is important for telomere elongation. Recruitment of telomerase to the double-stranded part of the telomere may anticipate its catalytic action at the 3′ end, perhaps by increasing the local concentration of telomerase. Importantly, the previously described S-phase-specific trafficking of telomerase to telomeres (23, 43, 44) is TIN2-TPP1 dependent (Fig. 1D and E), indicating that TIN2-TPP1-mediated recruitment is regulated by the cell cycle. While we cannot formally exclude an independent role for TPP1 and/or TIN2 in telomerase recruitment (since depletion of one is accompanied by reduction of the other [Fig. 2A and B]), current knowledge about the organization of the shelterin complex supports cofunction in the form of TIN2-anchored TPP1 (16, 51). The significance of telomerase association with telomeres via TIN2-TPP1 is indicated by the recent identification of TIN2 mutations in patients suffering from the short telomere disease dyskeratosis congenita (39). Our findings suggest that inefficient telomerase recruitment might contribute to the pathogenesis of dyskeratosis congenita in these patients. It is not yet known whether additional factors are involved in TIN2-TPP1-mediated recruitment of telomerase to telomeres. It was previously demonstrated that TPP1 associates with telomerase in cell extracts (52); however, it is not clear whether TPP1 interacts directly with telomerase.

The results presented here support the emerging view that certain shelterin components act as both negative and positive regulators of telomerase function (14, 40, 48, 52). While collectively the shelterin proteins inhibit telomerase-telomere interactions, evidence indicates that particular telomere-associated proteins can also interact with and recruit telomerase. These proteins include Cdc13 (*Saccharomyces cerevisiae*), TEBP-beta (ciliates), and TPP1 (humans and other vertebrates [this study]) (9, 31, 35–37, 48, 52). Recent studies indicate that dynamic phosphorylation of these proteins switches them between negative and positive regulation of telomerase recruitment by modulating the ability of the protein to interact with specific partner proteins. For example, in yeast, phosphorylation of Cdc13 by CDK1 favors an interaction with the Est1 subunit of telomerase (telomerase recruitment) over interaction with Stn1/Ten1 proteins (end protection) (30, 45). Likewise, in ciliates, phosphorylation of TEBP-beta stimulates the function of the protein in telomerase recruitment and interferes with formation of a heterodimer with TEBP-alpha, which functions in telomere protection (36). TPP1 is a structural homolog of the ciliate TEBP-beta protein (48, 52) and contains a conserved serine-rich domain with several predicted Cdk2 phosphorylation sites (48, 52). Our findings establish TPP1 as a central factor in telomerase recruitment in humans. While depletion of TPP1 reduces telomerase recruitment (this study), it can also lead to telomerase-mediated telomere extension (33, 54), suggesting that TPP1 is also poised to function as part of telomerase repressing and activating complexes in humans. To fully understand the mechanisms that underlie telomerase recruitment and understand the positive and negative roles of TPP1, POT1, and other shelterin components in telomerase regulation, it will be important to delineate the various telomeric states, identify the components of telomerase that associate with TPP1 during recruitment, and investigate whether phosphorylation of TPP1 plays a role in the regulated recruitment of telomerase to telomeres.

ACKNOWLEDGMENTS

We thank Susan Smith for kindly providing us with the TIN2 antibodies and Peter Baumann and Titia de Lange for POT1 antibodies. We are grateful to David Hall (University of Georgia) for overseeing statistical analysis.

This work was supported by a grant from the National Cancer Institute (RO1 CA104676) to M.P.T. and R.M.T. and by a Swiss National Science Foundation grant, the European Community's Seventh Framework Programme FP7/2007-2011 (grant agreement number 200950), and a European Research Council advanced investigator grant (grant agreement number 232812) to J.L. Eladio Abreu was supported by an NIH (NRSA) Predoctoral Fellowship Award To Promote Diversity in Health-Related Research (F31GM087949).

REFERENCES

1. **Almeida, F., R. Saffrich, W. Ansorge, and M. Carmo-Fonseca.** 1998. Microinjection of anti-coilin antibodies affects the structure of coiled bodies. J. Cell Biol. **142:**899–912.
2. **Armanios, M. Y., J. J. Chen, J. D. Cogan, J. K. Alder, R. G. Ingersoll, C. Markin, W. E. Lawson, M. Xie, I. Vulto, J. A. Phillips III, P. M. Lansdorp, C. W. Greider, and J. E. Loyd.** 2007. Telomerase mutations in families with idiopathic pulmonary fibrosis. N. Engl. J. Med. **356:**1317–1326.
3. **Autexier, C., R. Pruzan, W. D. Funk, and C. W. Greider.** 1996. Reconstitution of human telomerase activity and identification of a minimal functional region of the human telomerase RNA. EMBO J. **15:**5928–5935.
4. **Azzalin, C. M., and J. Lingner.** 2006. The human RNA surveillance factor UPF1 is required for S phase progression and genome stability. Curr. Biol. **16:**433–439.
5. **Azzalin, C. M., P. Reichenbach, L. Khoriauli, E. Giulotto, and J. Lingner.** 2007. Telomeric repeat containing RNA and RNA surveillance factors at mammalian chromosome ends. Science **318:**798–801.
6. **Baumann, P., and T. Cech.** 2001. Pot1, the putative telomere end-binding protein in fission yeast and humans. Science **292:**1171–1175.
7. **Bodnar, A. G., M. Ouellette, M. Frolkis, S. E. Holt, C.-P. Chiu, G. B. Morin, C. B. Harley, J. W. Shay, S. Lichtsteinter, and W. E. Wright.** 1998. Extension of life-span by introduction of telomerase into normal human cells. Science **279:**349–352.
8. **Broccoli, D., A. Smogorzewska, L. Chong, and T. de Lange.** 1997. Human telomeres contain two distinct Myb-related proteins, TRF1 and TRF2. Nat. Genet. **17:**231–235.
9. **Chandra, A., T. R. Hughes, C. I. Nugent, and V. Lundblad.** 2001. Cdc13 both positively and negatively regulates telomere replication. Genes Dev. **15:**404–414.
10. **Cong, Y. S., W. E. Wright, and J. W. Shay.** 2002. Human telomerase and its regulation. Microbiol. Mol. Biol. Rev. **66:**407–425.
11. **Crabbe, L., R. E. Verdun, C. I. Haggblom, and J. Karlseder.** 2004. Defective telomere lagging strand synthesis in cells lacking WRN helicase activity. Science **306:**1951–1953.

12. **Cristofari, G., E. Adolf, P. Reichenbach, K. Sikora, R. M. Terns, M. P. Terns, and J. Lingner.** 2007. Human telomerase RNA accumulation in Cajal bodies facilitates telomerase recruitment to telomeres and telomere elongation. Mol. Cell **27:**882–889.
13. **Cristofari, G., and J. Lingner.** 2006. Telomere length homeostasis requires that telomerase levels are limiting. EMBO J. **25:**565–574.
14. **Cristofari, G., K. Sikora, and J. Lingner.** 2007. Telomerase unplugged. ACS Chem. Biol. **2:**155–158.
15. **d'Adda di Fagagna, F., P. M. Reaper, L. Clay-Farrace, H. Fiegler, P. Carr, T. Von Zglinicki, G. Saretzki, N. P. Carter, and S. P. Jackson.** 2003. A DNA damage checkpoint response in telomere-initiated senescence. Nature **426:** 194–198.
16. **de Lange, T.** 2005. Shelterin: the protein complex that shapes and safeguards human telomeres. Genes Dev. **19:**2100–2110.
17. **Denchi, E. L., and T. de Lange.** 2007. Protection of telomeres through independent control of ATM and ATR by TRF2 and POT1. Nature **448:** 1068–1071.
18. **Greider, C. W., and E. H. Blackburn.** 1989. A telomeric sequence in the RNA of Tetrahymena telomerase required for telomere repeat synthesis. Nature **337:**331–337.
19. **Guo, X., Y. Deng, Y. Lin, W. Cosme-Blanco, S. Chan, H. He, G. Yuan, E. J. Brown, and S. Chang.** 2007. Dysfunctional telomeres activate an ATM-ATR-dependent DNA damage response to suppress tumorigenesis. EMBO J. **26:**4709–4719.
20. **Hockemeyer, D., W. Palm, T. Else, J. P. Daniels, K. K. Takai, J. Z. Ye, C. E. Keegan, T. de Lange, and G. D. Hammer.** 2007. Telomere protection by mammalian Pot1 requires interaction with Tpp1. Nat. Struct. Mol. Biol. **14:**754–761.
21. **Hockemeyer, D., A. J. Sfeir, J. W. Shay, W. E. Wright, and T. de Lange.** 2005. POT1 protects telomeres from a transient DNA damage response and determines how human chromosomes end. EMBO J. **24:**2667–2678.
22. **Jady, B. E., E. Bertrand, and T. Kiss.** 2004. Human telomerase RNA and box H/ACA scaRNAs share a common Cajal body-specific localization signal. J. Cell Biol. **164:**647–652.
23. **Jady, B. E., P. Richard, E. Bertrand, and T. Kiss.** 2006. Cell cycle-dependent recruitment of telomerase RNA and Cajal bodies to human telomeres. Mol. Biol. Cell **17:**944–954.
24. **Kibe, T., G. A. Osawa, C. E. Keegan, and T. de Lange.** 2010. Telomere protection by TPP1 is mediated by POT1a and POT1b. Mol. Cell. Biol. **30:**1059–1066.
25. **Kim, S. H., C. Beausejour, A. R. Davalos, P. Kaminker, S. J. Heo, and J. Campisi.** 2004. TIN2 mediates functions of TRF2 at human telomeres. J. Biol. Chem. **279:**43799–43804.
26. **Kondo, T., N. Oue, K. Yoshida, Y. Mitani, K. Naka, H. Nakayama, and W. Yasui.** 2004. Expression of POT1 is associated with tumor stage and telomere length in gastric carcinoma. Cancer Res. **64:**523–529.
27. **Lansdorp, P. M.** 2009. Telomeres and disease. EMBO J. **28:**2532–2540.
28. **Latrick, C. M., and T. R. Cech.** 2010. POT1-TPP1 enhances telomerase processivity by slowing primer dissociation and aiding translocation. EMBO J. **29:**924–933.
29. **Lei, M., E. R. Podell, and T. R. Cech.** 2004. Structure of human POT1 bound to telomeric single-stranded DNA provides a model for chromosome end-protection. Nat. Struct. Mol. Biol. **11:**1223–1229.
30. **Li, S., S. Makovets, T. Matsuguchi, J. D. Blethrow, K. M. Shokat, and E. H. Blackburn.** 2009. Cdk1-dependent phosphorylation of Cdc13 coordinates telomere elongation during cell-cycle progression. Cell **136:**50–61.
31. **Lin, J. J., and V. A. Zakian.** 1996. The *Saccharomyces CDC13* protein is a single-strand TG_{1-3} telomeric DNA-binding protein *in vitro* that affects telomere behavior *in vivo*. Proc. Natl. Acad. Sci. U. S. A. **93:**13760–13765.
32. **Lingner, J., T. R. Hughes, A. Sherchenko, M. Mann, V. Lundblad, and T. R. Cech.** 1997. Reverse transcriptase motifs in the catalytic subunit of telomerase. Science **276:**561–567.
33. **Liu, D., A. Safari, M. S. O'Connor, D. W. Chan, A. Laegeler, J. Qin, and Z. Songyang.** 2004. PTOP interacts with POT1 and regulates its localization to telomeres. Nat. Cell Biol. **6:**673–680.
34. **Loayza, D., and T. De Lange.** 2003. POT1 as a terminal transducer of TRF1 telomere length control. Nature **424:**1013–1018.
35. **Nugent, C. I., T. R. Hughes, N. F. Lue, and V. Lundblad.** 1996. Cdc13p: a single-strand telomeric DNA-binding protein with a dual role in yeast telomere maintenance. Science **274:**249–252.
36. **Paeschke, K., S. Juranek, T. Simonsson, A. Hempel, D. Rhodes, and H. J. Lipps.** 2008. Telomerase recruitment by the telomere end binding protein-beta facilitates G-quadruplex DNA unfolding in ciliates. Nat. Struct. Mol. Biol. **15:**598–604.
37. **Paeschke, K., T. Simonsson, J. Postberg, D. Rhodes, and H. J. Lipps.** 2005. Telomere end-binding proteins control the formation of G-quadruplex DNA structures in vivo. Nat. Struct. Mol. Biol. **12:**847–854.
38. **Palm, W., and T. de Lange.** 2008. How shelterin protects mammalian telomeres. Annu. Rev. Genet. **42:**301–334.
39. **Savage, S. A., N. Giri, G. M. Baerlocher, N. Orr, P. M. Lansdorp, and B. P. Alter.** 2008. TINF2, a component of the shelterin telomere protection complex, is mutated in dyskeratosis congenita. Am. J. Hum. Genet. **82:**501–509.
40. **Smogorzewska, A., and T. De Lange.** 2004. Regulation of telomerase by telomeric proteins. Annu. Rev. Biochem. **73:**177–208.
41. **Smogorzewska, A., B. van Steensel, A. Bianchi, S. Oelmann, M. R. Schaefer, G. Schnapp, and T. de Lange.** 2000. Control of human telomere length by TRF1 and TRF2. Mol. Cell. Biol. **20:**1659–1668.
42. **Takai, H., A. Smogorzewska, and T. de Lange.** 2003. DNA damage foci at dysfunctional telomeres. Curr. Biol. **13:**1549–1556.
43. **Tomlinson, R. L., E. B. Abreu, T. Ziegler, H. Ly, C. M. Counter, R. M. Terns, and M. P. Terns.** 2008. Telomerase reverse transcriptase is required for the localization of telomerase RNA to cajal bodies and telomeres in human cancer cells. Mol. Biol. Cell **19:**3793–3800.
44. **Tomlinson, R. L., T. D. Ziegler, T. Supakorndej, R. M. Terns, and M. P. Terns.** 2006. Cell cycle-regulated trafficking of human telomerase to telomeres. Mol. Biol. Cell **17:**955–965.
45. **Tseng, S. F., Z. J. Shen, H. J. Tsai, Y. H. Lin, and S. C. Teng.** 2009. Rapid Cdc13 turnover and telomere length homeostasis are controlled by Cdk1-mediated phosphorylation of Cdc13. Nucleic Acids Res. **37:**3602–3611.
46. **Venteicher, A. S., E. B. Abreu, Z. Meng, K. E. McCann, R. M. Terns, T. D. Veenstra, M. P. Terns, and S. E. Artandi.** 2009. A human telomerase holoenzyme protein required for Cajal body localization and telomere synthesis. Science **323:**644–648.
47. **Vulliamy, T. J., and I. Dokal.** 2008. Dyskeratosis congenita: the diverse clinical presentation of mutations in the telomerase complex. Biochimie **90:**122–130.
48. **Wang, F., E. R. Podell, A. J. Zaug, Y. Yang, P. Baciu, T. R. Cech, and M. Lei.** 2007. The POT1-TPP1 telomere complex is a telomerase processivity factor. Nature **445:**506–510.
49. **Weinrich, S. L., R. Pruzan, L. Ma, M. Ouellette, V. M. Tesmer, S. E. Holt, A. G. Bodnar, S. Lichtsteiner, N. W. Kim, J. B. Trager, R. D. Taylor, R. Carlos, W. H. Andrews, W. E. Wright, J. W. Shay, C. B. Harley, and G. B. Morin.** 1997. Reconstitution of human telomerase with the template RNA component hTR and the catalytic protein subunit hTRT. Nat. Genet. **17:** 498–502.
50. **Wenz, C., B. Enenkel, M. Amacker, C. Kelleher, K. Damm, and J. Lingner.** 2001. Human telomerase contains two cooperating telomerase RNA molecules. EMBO J. **20:**3526–3534.
51. **Xin, H., D. Liu, and Z. Songyang.** 2008. The telosome/shelterin complex and its functions. Genome Biol. **9:**232.
52. **Xin, H., D. Liu, M. Wan, A. Safari, H. Kim, W. Sun, M. S. O'Connor, and Z. Songyang.** 2007. TPP1 is a homologue of ciliate TEBP-beta and interacts with POT1 to recruit telomerase. Nature **445:**559–562.
53. **Ye, J. Z., and T. de Lange.** 2004. TIN2 is a tankyrase 1 PARP modulator in the TRF1 telomere length control complex. Nat. Genet. **36:**618–623.
54. **Ye, J. Z., D. Hockemeyer, A. N. Krutchinsky, D. Loayza, S. M. Hooper, B. T. Chait, and T. de Lange.** 2004. POT1-interacting protein PIP1: a telomere length regulator that recruits POT1 to the TIN2/TRF1 complex. Genes Dev. **18:**1649–1654.
55. **Yehezkel, S., Y. Segev, E. Viegas-Pequignot, K. Skorecki, and S. Selig.** 2008. Hypomethylation of subtelomeric regions in ICF syndrome is associated with abnormally short telomeres and enhanced transcription from telomeric regions. Hum. Mol. Genet. **17:**2776–2789.
56. **Zhu, Y., R. L. Tomlinson, A. A. Lukowiak, R. M. Terns, and M. P. Terns.** 2004. Telomerase RNA accumulates in Cajal bodies in human cancer cells. Mol. Biol. Cell **15:**81–90.